ELSEVIER

Technical note

Measurement of the optical extinction coefficient of combustion-generated aerosol

John F. Widmann[*], Jason Duchez[1], Jiann C. Yang[2], Joseph M. Conny[3],
George W. Mulholland[2]

National Institute of Standards and Technology, 100 Bureau Drive, Gaithersburg, MD 20899, USA

Abstract

This note describes measurements of the mass-specific extinction coefficient, σ_s, of carbonaceous aerosol produced during hydrocarbon combustion. Measurements of σ_s were obtained by laser extinction at $\lambda = 632$ nm. The aerosol was generated using a laminar diffusion flame, and the mass-specific extinction coefficient determined as a function of the global equivalence ratio, ϕ. The elemental carbon content of the aerosol was also determined with respect to ϕ. A relationship was developed between the elemental carbon/total carbon (EC/TC) ratio and σ_s. A simple method of producing laboratory aerosol with controlled EC/TC ratio is also presented.
Crown Copyright © 2004 Published by Elsevier Ltd. All rights reserved.

Keywords: Soot; Smoke; Extinction coefficient; Carbonaceous aerosol; Elemental carbon; Total carbon

1. Background

This note describes experiments in which the mass-specific extinction coefficient, σ_s, of carbonaceous aerosol was correlated with the fraction of elemental carbon present in the aerosol (EC/TC ratio). Here,

---

[*] Corresponding author. Current affiliation: Fluent, Inc., 10 Cavendish Court, Lebanon, NH 03766, USA. Tel.: +1 603 643 2600; fax: +1 603 643 3967.

  E-mail address: jfw@fluent.com (J.F. Widmann).

  [1] Also affiliated with the Department of Physics, University of Maryland, College Park, MD, USA.

  [2] Building and Fire Research Laboratory.

  [3] Chemical Science and Technology Laboratory.

it is assumed that carbon present in the aerosol that is not organic carbon is elemental carbon, which is defined as light-absorbing (or black) carbon.

The transmission, τ, of radiation through an aerosol dispersion (neglecting absorption due to the continuous phase) can be quantified using the expression

$$\tau = \frac{I}{I_0} = \exp(-\sigma_s m_s L), \tag{1}$$

where I_0 and I correspond to the incident and transmitted radiant intensities, respectively. Here, m_s is the mass of aerosol per unit volume and L is the path length. In general, σ_s may be a function of the radiation wavelength, λ, and the aerosol properties (chemical composition, temperature, morphology, and size distribution). Application of Eq. (1) requires that the aerosol dispersion be homogeneous along the optical path.

In theory, one can predict the mass-specific extinction coefficient from knowledge of the aerosol refractive index and a suitable model of the scattering and absorption of radiation by the particles. In the case of carbonaceous aerosol particles, however, this is complicated by large uncertainties in the refractive index and morphology of the particles (Dalzell & Sarofim, 1969; Lee & Tien, 1981). Recently generated particles have fractal-like agglomerate structures for which light-scattering models have not yet been sufficiently validated (Felske et al., 1984; Habib & Vervisch, 1988; Charalampopoulos et al., 1989), while aged aerosol can have organic and aqueous material adsorbed on the particle resulting in an unknown mixing state (Fuller et al., 1999; Jacobson, 2000; Hasegawa & Ohta, 2002; Jacobson, 2002). Rayleigh theory (van de Hulst, 1957) is frequently used to predict the extinction of visible and infrared radiation due to soot particles; however, significant uncertainties result from combining such a simple theory with measured optical constants containing large uncertainties themselves. For example, using Rayleigh theory with the values of the complex refractive index reported by Dalzell and Sarofim (1969), the predicted values of the mass-specific extinction coefficient, σ_s, for acetylene and propane at $\lambda = 0.649\,\mu m$ are 3.2 and $3.8\,m^2\,g^{-1}$, respectively. For comparison, Mulholland and Croarkin (2000) reported that $\sigma_s = 8.7\,m^2\,g^{-1}$ was the best estimate of the mean value determined from a literature search of experimental measurements (various fuels) obtained at $\lambda = 0.633\,\mu m$, which is more than twice the predicted values. As such, direct experimental measurement is currently a preferable approach to determining the mass-specific extinction coefficient of combustion-generated particles.

2. Experimental

2.1. Optical extinction measurements

The experimental apparatus used for the optical extinction measurements is shown schematically in Fig. 1. The soot aerosol was generated in a laminar diffusion burner, diluted with nitrogen, and carried by the combustion gases and N_2 to the optical cell. The apparatus was equipped with filters to remove particles from the gas stream prior to the measurement, or to measure gravimetrically the mass of soot aerosol present upstream and downstream of the optical cell. A settling cell was also in-line to remove the largest soot agglomerates from the aerosol. The sedimentation cell was to reduce soot deposition in
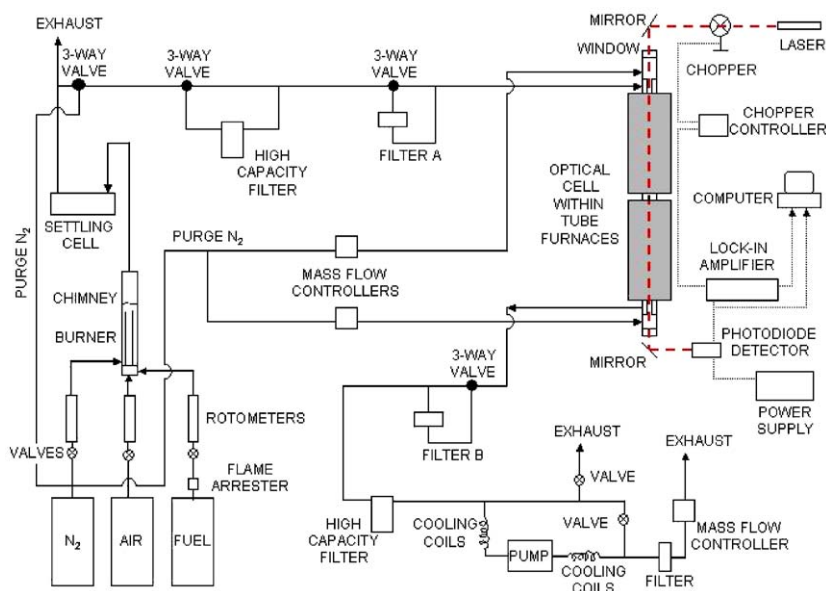
Fig. 1. Experimental apparatus used for the optical extinction measurements.

the optical cell and associated tubing. Downstream of the optical cell, the particles were filtered from the gas stream prior to the gas entering the pump.

The laminar diffusion burner consisted of two concentric tubes, with fuel and air flowing through the inner and outer tubes, respectively. The data presented here correspond to experiments in which ethene was used as the fuel, although it has been shown previously that hydrocarbon fuels tend to produce soot aerosol with similar mass-specific extinction coefficients (Smyth & Shaddix, 1996; Widmann et al., 2003; Widmann, 2003). The fuel-flow rate was maintained at 4.5 $cm^3 s^{-1}$, and the air was varied to control the global equivalence ratio. The inner diameters of the fuel and air tubes were 9 and 35 mm, respectively. The combustion products flowed through a Pyrex[4] tube with an inner diameter of 26 mm that extends 27 cm downstream of the fuel and air ducts. An outer Pyrex tube surrounded the 27 cm long Pyrex tube as shown in Fig. 1. This outer tube had an inner diameter of 50 mm and extended 61 cm downstream of the fuel and air ducts. Nitrogen (180 $cm^3 s^{-1}$) was added between the inner and outer Pyrex tubes to dilute the aerosol downstream of the inner Pyrex tube. A tripper plate located 30 cm downstream of the fuel and air ducts was used to instigate turbulent mixing and to produce a more homogeneous aerosol dispersion (Leonard et al., 1994). Prior to the tripper plate, the flame was laminar and steady.

The optical cell consisted of a quartz tube situated within two tube furnaces as shown in Fig. 1. The quartz tube was designed with removable windows and air purges at the top and bottom to prevent soot particles from depositing on the windows. The path length between the two purge lines is 57.8 cm. The flow rates of the top and bottom air purges were maintained at 2.2 and 2.4 $cm^3 s^{-1}$, respectively. Mass flow

---

[4] Certain commercial equipment, instruments, or materials are identified in this paper to specify adequately the experimental procedure. Such identification does not imply recommendation or endorsement by the National Institute of Standards and Technology, nor does it imply that the materials or equipment are necessarily the best available for this purpose.

controllers were used to regulate the gas flow rate through the optical cell ($144 \, cm^3 \, s^{-1}$) and purge lines. The tube furnaces were set at $60 \, °C$ to prevent moisture condensation on the particles. The maximum dew-point temperature was calculated to be $27.5 \, °C$ assuming complete combustion under stoichiometric conditions.

The extinction measurements were obtained using a solid-state laser operating at $632 \, nm$ and a photodiode to measure the laser light intensity. A chopper and lock-in amplifier were used to minimize background signal and permit measurements at elevated temperatures (not presented here). The calculation of σ_s requires the determination of the concentration on a mass basis of the aerosol dispersion, m_s, as shown in Eq. (1). The mass concentration of particles in the optical cell was determined gravimetrically by alternately collecting the soot on teflon filters upstream and downstream of the optical cell. The filters used for the gravimetric measurements are labeled filter A and filter B in Fig. 1. These filters have a reported collection efficiency of 99% for particles larger than $0.1 \, \mu m$. Additional details of the gravimetric measurements have been reported elsewhere (Mulholland & Choi, 1998).

2.2. EC/TC measurements

Elemental carbon mass was measured by the thermal-optical transmission (TOT) method employed with the Sunset Laboratories' thermal optical carbon analyzer. Briefly, refractory elemental carbon, or elemental carbon (EC), is distinguished from aerosol organic carbon (OC) through a protocol of thermal desorption accompanied by pyrolysis in helium followed by thermal oxidation in a flow with a volume fraction of 1% of O_2 in He. As carbon evolves from a filter sample, it is reduced downstream and detected by flame ionization detection. Pyrolysis of OC generates char, which is indicated by the attenuation of $670 \, nm$ laser light. EC is differentiated from OC when the attenuated laser signal returns to the level prior to the initiation of the heating protocol, indicating that an amount of carbon equivalent to the original OC component has been removed from the filter sample and only the carbon mass equivalent to EC remains. Further thermal oxidation in He–O_2 removes the native EC, which is subsequently reduced downstream and detected by flame ionization detection. Total carbon (TC) is the sum of OC and native EC. For these measurements, quartz fiber filters were used (Pallflex Tissuequartz 2500 QAT-UP).

The protocol for thermal desorption, pyrolysis, and thermal oxidation of aerosol carbon used here is based upon a protocol developed at NIST which optimized TOT for accuracy in measuring refractory light-absorbing carbon (Conny et al., 2003). Thermal desorption and pyrolysis of OC occurred as the sample was heated in helium during a sequence of four temperature steps: (1) $190 \, °C$ for $60 \, s$, (2) $365 \, °C$ for $60 \, s$, (3) $610 \, °C$ for $60 \, s$, and (4) $835 \, °C$ for $72 \, s$. Immediately following the He phase, remaining aerosol carbon was thermally oxidized in He–O_2 as the sample was heated in four additional temperature steps: (1) $550 \, °C$ for $120 \, s$, (2) $700 \, °C$ for $60 \, s$, (3) $850 \, °C$ for $60 \, s$, and (4) $940 \, °C$ for $300 \, s$.

3. Results

Fig. 2 presents the measured mass-specific extinction coefficient with respect to the global equivalence ratio, ϕ. The equivalence ratio is defined as the fuel–air ratio normalized by the fuel–air ratio under stoichiometric conditions. The error bars presented in the figure represent the statistical variation in the measurements and were calculated as twice the standard error of the mean. Fig. 2 indicates that the
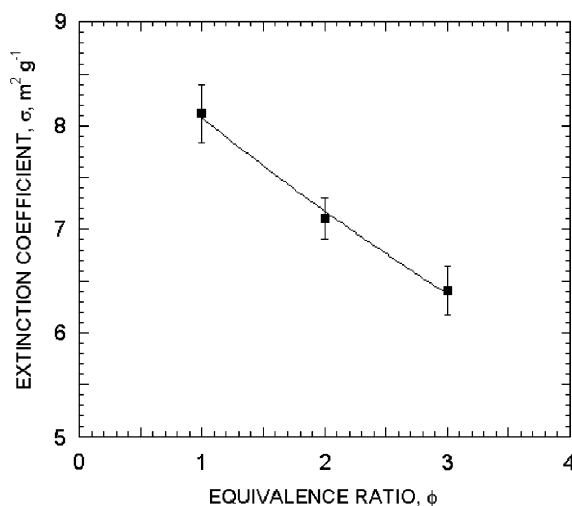
Fig. 2. Mass-specific extinction coefficient, σ_s, with respect to the global equivalence ratio, ϕ, at 632 nm.

mass-specific extinction coefficient decreases with increasing values of ϕ, which corresponds to under-ventilated combustion. This is consistent with the results of Mulholland and Croarkin (2000) and Widmann et al. (2003). It was shown previously that the mass-specific extinction coefficient for over-ventilated combustion ($\phi < 1$) does not change significantly from the stoichiometric case, and the differences are within the uncertainty of the measurement (Widmann et al., 2003; Smyth & Shaddix, 1996, and references cited therein). The solid line in Fig. 2 is an exponential fit to the data of the form

$$\sigma_s = \alpha_\sigma \exp(-\beta_\sigma \phi), \tag{2}$$

where $\alpha_\sigma = 9.09 \, \text{m}^2 \, \text{g}^{-1}$ and $\beta_\sigma = 0.118$. The exponential fit, which has a correlation coefficient of 0.997, will be used below to relate the mass-specific extinction coefficient to the elemental carbon/total carbon (EC/TC) ratio of the aerosol.

In addition to the extinction measurements presented in Fig. 2, measurements of the EC/TC ratio of the aerosol were also obtained. Fig. 3 presents the measured values of the EC/TC ratio with respect to the global equivalence ratio. A thorough uncertainty analysis of the EC/TC measurements was not conducted; however, Conny et al. (2003) reported a relative standard uncertainty of 1.7% for urban particulate matter with a high EC content using the thermal desorption protocol used here. This uncertainty is believed to be relevant to the measurements presented here. Like the mass-specific extinction coefficient, the EC/TC ratio is also found to decrease with increasing values of ϕ. This is consistent with the findings of Leonard et al. (1994), who noted that under-ventilated combustion leads to aerosol particles with higher organic content relative to stoichiometric and over-ventilated combustion. The solid line in Fig. 3 is an exponential fit to the data of the form

$$EC/TC = \alpha_c \exp(-\beta_c \phi), \tag{3}$$

where $\alpha_c = 1.165$ and $\beta_c = 0.329$. The curve fit to the experimental data in Fig. 3 has a correlation coefficient of 0.991, and represents the effect of the global equivalence ratio on the fraction of elemental carbon in the particles.
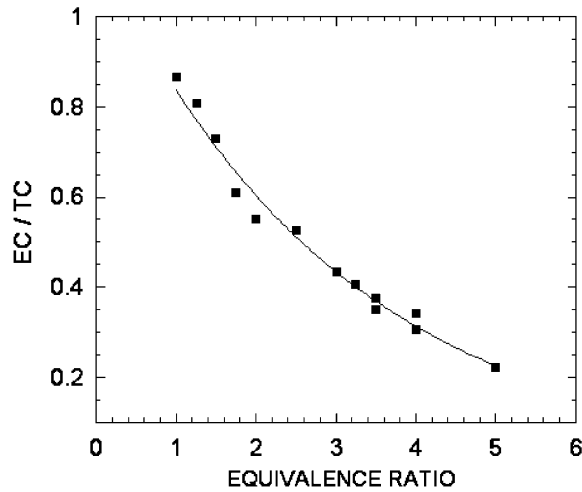
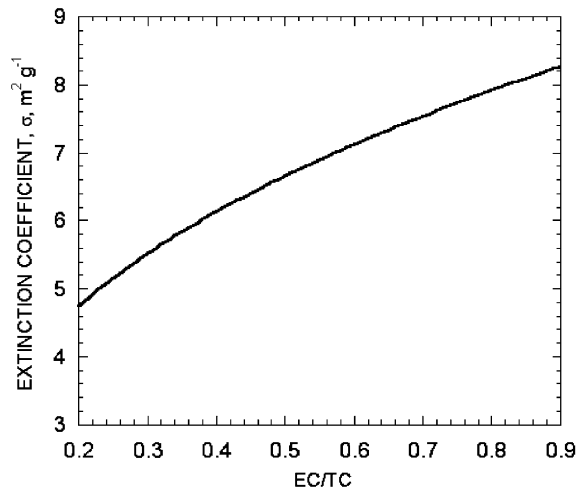Fig. 3. Ratio of elemental carbon to total carbon (EC/TC) with respect to the global equivalence ratio, ϕ.

Fig. 4. Relationship between the mass-specific extinction coefficient, σ_s, and the EC/TC ratio at 632 nm.

Combining Eqs. (2) and (3) to eliminate the global equivalence ratio yields

$$\sigma_s = \alpha_\sigma \left[\frac{EC/TC}{\alpha_c} \right]^{(\beta_\sigma/\beta_c)} = 8.6(EC/TC)^{0.36}, \tag{4}$$

which relates the mass-specific extinction coefficient to the EC/TC ratio. The values of σ_s obtained from Eq. (4) are shown in Fig. 4 for EC/TC ratios ranging from 0.2 to 0.9. Note that the EC/TC measurements presented in Fig. 3 cover the range $0.2 < EC/TC < 0.9$; however, the extinction measurements in Fig. 2 only cover the range $6.4\,m^2\,g^{-1} < \sigma_s < 8.1\,m^2\,g^{-1}$. Thus, the relationship presented in Fig. 4 extrapolates the curve fits beyond the σ_s data at both ends.

4. Summary

A relationship between the mass-specific extinction coefficient of combustion-generated aerosol and the EC/TC ratio of the aerosol is presented. The mass-specific extinction coefficient was found to increase with increasing values of the EC/TC ratio. The experimental apparatus used also provides a simple method of generating laboratory aerosol with controlled EC/TC ratios.

References

Charalampopoulos, T. T., Chang, H., & Stagg, B. (1989). The effects of temperature and composition on the complex refractive index of flame soot. *Fuel*, *68*, 1173–1179.

Conny, J. M., Klinedinst, D. B., Wight, S. A., & Paulsen, J. L. (2003). Optimizing thermal–optical methods for measuring atmospheric elemental (black) carbon: A response surface study. *Aerosol Science of Technology*, *37*, 703–723.

Dalzell, W. H., & Sarofim, A. F. (1969). Optical constants of soot and their application to heat-flux calculations. *Journal of Heat Transfer*, *91*, 100–104.

Felske, J. D., Charalampopoulos, T. T., & Hura, H. S. (1984). Determination of the refractive indices of soot particles from the reflectivities of compressed soot pellets. *Combustion Science and Technology*, *37*, 263–283.

Fuller, K. A., Malm, W. C., & Kreidenweis, S. M. (1999). Effects of mixing on extinction by carbonaceous particles. *Journal of Geophysical Research*, *104*, 15941–15954.

Habib, Z. G., & Vervisch, P. (1988). On the refractive index of soot at flame temperature. *Combustion Science and Technology*, *59*, 261–274.

Hasegawa, S., & Ohta, S. (2002). Some measurements of the mixing state of soot-containing particles at urban and non-urban sites. *Atmospheric Environment*, *36*, 3899–3908.

Jacobson, M. Z. (2000). A physically-based treatment of elemental carbon optics: Implications for global direct forcing of aerosols. *Geophysical Research Letters*, *27*, 217–220.

Jacobson, M. Z. (2002). Control of fossil–fuel particulate elemental carbon and organic matter, possibly the most effective method of slowing global warming. *Journal of Geophysical Research*, *107*, 4410–4431.

Lee, S. C., & Tien, C. L. (1981). Optical constants of soot in hydrocarbon flames. *Eighteenth symposium* (*international*) *on combustion* (pp. 1159–1166). The Combustion Institute.

Leonard, S., Mulholland, G. W., Puri, R., & Santoro, R. J. (1994). Generation of CO and smoke during under-ventilated combustion. *Combustion and Flame*, *98*, 20–34.

Mulholland, G. W., & Choi, M. Y. (1998). Measurement of the mass-specific extinction coefficient for acetylene and ethane smoke using the large agglomerate optics facility. *Twenty-seventh symposium* (*International*) *on combustion* (pp. 1515–1522). The Combustion Institute.

Mulholland, G. W., & Croarkin, C. (2000). Specific extinction coefficient of flame generated smoke. *Fire and Materials*, *24*, 227–230.

Smyth, K. C., & Shaddix, C. R. (1996). The elusive history of $m = 1.57 - 0.56i$ for the refractive index of soot. *Combustion and Flame*, *107*, 314–320.

van de Hulst, H. C. (1957). Light scattering by small particles. Toronto, Ontario: General Publishing Company, Ltd.

Widmann, J. F. (2003). Evaluation of the Planck mean absorption coefficients for radiation transport through smoke. *Combustion Science and Technology*, *175*, 2299–2308.

Widmann, J. F., Yang, J. C., Smith, T. J., Manzello, S. L., & Mulholland, G. W. (2003). Measurement of the optical extinction coefficients of post-flame soot in the infrared. *Combustion and Flame*, *134*, 119–129.